Immunity, Volume *54*

Supplemental information

Prenatal interleukin 6 elevation increases glutamatergic synapse density and disrupts hippocampal connectivity in offspring

Filippo Mirabella, Genni Desiato, Sara Mancinelli, Giuliana Fossati, Marco Rasile, Raffaella Morini, Marija Markicevic, Christina Grimm, Clara Amegandjin, Alberto Termanini, Clelia Peano, Paolo Kunderfranco, Graziella di Cristo, Valerio Zerbi, Elisabetta Menna, Simona Lodato, Michela Matteoli, and Davide Pozzi

SUPPLEMENTARY FIGURE LEGENDS

Figure S1 refers to Figure 1: Transient prenatal elevation of IL-6 disrupts normal brain network connectivity within specific large-scale circuits and alters spatial memory.

(A) Representative scheme showing the experimental procedure used for the in vivo approach: a single pulse of either vehicle (saline, as control) or IL-6 (5μg) was intraperitoneally injected in pregnant mothers at gestational day 15 and the male offspring were analyzed at different post-natal day with different experimental techniques.

(B) Immunofluorescence analysis of VGLUT1 and VGAT positive puncta in CA1 hippocampal neurons at P30 in the two conditions. Scale Bar 10μm.

(C) Quantitative analysis of VGLUT1 and VGAT area (vehicle n=7 male mice; IL-6 n=6 male mice.; Three independent experiments, Mann-Whitney test, **p=0,0047).

(D) (Upper panel) Scheme of the experimental set-up for MRI recordings. Adult male offspring from mothers exposed to IL-6 or Vehicle at GD15 underwent a single MRI session to record resting-state fMRI and diffusion tensor imaging, under light anesthesia (isoflurane 0.5% + medetomidine 0.1 mg/kg/h). (Lower Panel) Circos-plot showing the anatomical location of hypo-connected edges (n=36) in IL-6 mice compared to vehicle-treated mice ($p<0.05$, uncorrected).

(E) Dual-regression analysis in 15 resting-state networks (RSNs) revealed a significant increase only in the Dorsal Hippocampal network strength in the IL-6 group compared to vehicle mice. Multivariate ANOVA, Bonferroni corrected across 15 RSNs.

(F) Fractional anisotropy (FA) was assessed by diffusion tensor imaging and quantified in nine large white matter structures. None of these structures show significant microstructural differences between IL-6 and vehicle-treated mice. Multivariate ANOVA, Bonferroni corrected across 9 structures.

(G-H) Discrimination *index* values in novel object location (G) and in novel object recognition (H). Vehicle n=10 male mice, IL-6 n=14 male mice from 2 independent mothers. *p=0,043 Unpaired t test with Welch's correction.

(I) Elevated plus maze: quantification of the percentage of time spent in the closed and open arms of plus maze arena.

(J) Open field: Quantification of distance travelled separately in the center and periphery, and total distance (cm) in an open field arena. Two-way Anova with Sidak's multiple comparison Post hoc test. Vehicle n=13 male mice, IL-6 n=7 male mice, from three independent mothers.

Figure S2 refers to Figure 1: Transient prenatal elevation of IL-6 does not alter the gross anatomy and the glial composition of the brain in offspring

(A). Nissl staining of three independent P15 brain coronal sections, at different rostro-caudal levels, derived from mice prenatally exposed to Vehicle- or IL-6 via maternal intraperitoneal injection. Scale bar 500 µm. Ctx: Cortex, Str: Striatum, Hp: Hippocampus. LV: Later Ventricle. No gross anatomical malformations are present.

(B). Representative image of P30 coronal brain sections stained for Satb2 (green), NeuroD2 (red), NeuN (grey) Hoechst (blue), obtained from mice prenatally exposed to either Vehicle or IL-6. Scale bar 1000 µm. Relative image of the selected (dashed rectangle) area of the somatosensory cortex showed below. Scale bar 500 µm. Right panel: quantitative analysis of SATB2 intensity (Vehicle n= 4 mice, IL-6 n= 4 mice. Two independent experiments).

(C) Immunofluorescence analysis of coronal brain section at P15 in CA1 hippocampal region, obtained from mice prenatally exposed to vehicle- or IL-6 via maternal intraperitoneal injection, stained with Hoechst (blue), GFAP (red), and NeuN (White). Scale bar 50 µm.

(D) Quantitative analysis of astrocyte properties (left panels) including GFAP mean intensity and astrocyte density (Vehicle n=6 mice, IL-6 n=6 mice. Two independent experiments).

(E) Immunofluorescence analysis of Immunofluorescence analysis of coronal brain section at P15 in CA1 hippocampal and (F) cortical region, obtained from mice prenatally exposed to Vehicle- or IL-6 via maternal intraperitoneal injection stained with Iba1 (green), NeuN (white) and Hoechst (blue).

(G-H) Quantitative analysis of microglia morphological features (ramification, Cell territory, number of branching, branch length), intensity of Iba1 and microglia density in both hippocampus (G) and cortex (H) of mice prenatally exposed to IL-6 or vehicle. (Vehicle n=6 mice, IL-6 n=6 mice. Two independent experiments).

(I-J) gene expression analysis through qPCR of a panel of inflammation-derive molecules performed in hippocampus (I) and cortex (J) of mice prenatally exposed to IL-6 or vehicle (Vehicle n=16 mice, IL-6 n=18 mice. Three independent experiments).

Figure S3 refers to Figure 2. Single cell sequencing in hippocampi at E16 exposed to IL-6 at E15

(A) UMAP colored by sample type and cell types divided by treatment.

(B) Histogram plot showing the cell type proportion in the two experimental groups.

(C) Violin Plots showing QC parameters used in the analysis pipeline: nCount_RNA, raw read count per cells; nFaturre_RNA, number of gene per cell; MTPCY; percent of mitochondrial genes per cell.

(D) Venn diagram showing the degree of overlaps between cell types of differentially expressed genes upon IL-6 treatment.

(E) Volcano plot showing DEGs in DE-EXN cell type.

(F) Bar plot showing enriched gene ontology in DE-ExN DEGs.

Figure S4 refers to Figure 3: Chronic IL-6 treatment in cultured neurons does not increase GABAergic synapses and does not alter neither presynaptic release probability nor electrically evoked neuronal calcium transients.

(A) (Left panel) Quantitative analysis of resting potential measured in current clamp configuration (I=0) in untreated and chronically treated neurons with IL-6 10 ng/ml. (Right panel) Quantitative analysis of membrane resistance measured in voltage clamp configuration in untreated and chronically treated neurons with IL-6 10 ng/ml (Resting Potential: Ctrl n=26 cells, IL-6 n=23 cells. Input Resistance: Ctrl n= 33 cells, IL-6 n= 31 cells. Three independent experiments).

(B) Immunofluorescence analysis of cultured hippocampal neurons at 14 DIV stained with b3Tubulin (green), Gephyrin (red), VGAT (white) in control condition or upon IL-6 treatment.

(C) Quantification of Gephyrin and VGAT colocalizing puncta per 10 μm length of β3Tubulin in both conditions. (Ctrl n=102, IL-6 n= 112. Four independent experiments).

(D) Representative electrophysiological traces of excitatory post-synaptic currents (EPSC) evoked by paired pulse at 50 msec both in control condition and upon IL-6 chronic treatment at 10 ng/ml.

(E) Short term plasticity measured as paired pulse ratio (PPR) between first and second EPSC evoked at different interpulse intervals. (Ctrl n=15 cells, IL-6 n=15 cells. Three independent experiments).

(F) Quantitative analysis of a single electrically evoked EPSC recorded in the two conditions. (Ctrl n=42 cells, IL-6 n= 42 cells. Three independent experiments, Mann-Whitney test. *p<0,0138).

(G) Upper panels: Pseudocolor images of cultured neurons in control condition loaded with calcium sensitive dye Oregon-Green and imaged (505 nm) in resting state (left panel) and upon an electrical field stimulation (90 mA for 2 sec @ 20Hz, right panel) in the present of synaptic transmission blockers (scale bar 50 μm). Lower panels: temporal analysis of intracellular calcium changes measured at somato-dendritic level during electrical stimulation in control (left) and IL6 (right) treated neurons.

(H) Quantitative analyses of intracellular calcium influx in control condition and upon chronic IL-6 10 ng/ml treatment. (number of analyzed cells: Ctrl n=184, IL-6 n=212. Three independent experiments).

(I) Immunofluorescence analysis of mature cultured neurons at 14 DIV stained with GFAP (red) NeuN (white) and Hoechst (blue) grown in control condition and upon increasing doses of Ara-C (1-4 μM), scale bar 100 μm.

(J) Quantitative analysis of the percentage of astrocytes (identified as GFAP-positive cells) and neurons (identified as NeuN-positive cells) in control cultured neurons and upon different concentrations of Ara-C at 14 DIV (Ctrl n= 24, Ara-C 1 μM n=23, Ara-C 2μM n=21, Ara-C 3μM n=21, Ara-C 4μM n=21. Two independent experiments. Kruskal-Wallis test followed by Dunn's multiple comparisons test. Neurons: Ara-C 1μM ***p=0,00039, Ara-C 2μM ****p=1,58x10^{-6}, Ara-C 3μM ****p=1,71x10^{-10}, Ara-C 4μM p<0,8x10^{-14}; Astrocytes: Ara-C 1μM ****p=1,46x10^{-5}, Ara-C 2μM ****p=5,19x10^{-6}, Ara-C 3μM ****p=6,59x10^{-10}, Ara-C 4μM ****p=3,6x10^{-14}).

(K) Quantitative analysis of the percentage of astrocytes (identified as GFAP-positive cells) and neurons (identified as NeuN-positive cells) in control cultured neurons at 1 and 7 DIV, and upon different concentrations of Ara-C (1 DIV n= 15, 7 DIV n=29, Ara-C 1 μM n=11, Arac-C 2μM n=11, Ara-C 3μM n=11, Ara-C 4μM n=12. One experiment. Kruskal-Wallis test followed by Dunn's multiple comparisons test. Neurons: 7DIV **** p=1,27x10^{-10}, Ara-C 1 μM* p=0,013, Ara-C 2 μM ** p=0,0088, Ara-C 3 μM **** p=7,81x10^$^{-8}$, Ara-C 4 μM ****p= 9,40x10^{-9}; Astrocytes: 7DIV **** p=3,58x10^{-10}, Ara-C 1 μM* p=0,027, Ara-C 2 μM ** p=0,0069 , Ara-C 3 μM **** p=8,2x10^{-9} , Ara-C 4 μM ****p=5,37x10^{-10}).

(L) Representative electrophysiological traces of mEPSC in Ara-C treated cultures both in control condition and upon the chronic treatment with IL-6 10 ng/ml. (Lowe panel) Quantitative analysis of amplitude and frequency of mEPSC in Ara-C treated neurons in both control and IL-6 treated neurons. (Ctrl n= 24, IL-6 n= 30. Three independent experiments. Mann-Whitney test. ***p=0,0002; *p=0,0452).

(M) Immunofluorescence analysis of cultured neurons untreated and chronically treated with IL-6 10ng/ml, stained with antibodies against specific neuronal (NeuN, green) glial (GFAP, red) and a general cellular marker (Hoechst, blue). Scale Bar 100μm. (Lower panel, left). Quantification of the total number of cells identified through Hoechst staining. (Ctrl n=32 coverslips, IL-6 n=31 coverslips. Roughly 3-4 field analyzed for each coverslip. Three independent experiments. Mann-Whitney test). (Lower panel, right) Ratio in percentage of GFAP positive (astrocytes) to the NeuN positive (neurons) cells in the two conditions (Three independent experiments. Mann-Whitney test).

(N) Representative immunofluorescence images of cultured hippocampal neurons at 7 DIV stained with MAP2 (green), Iba1 (red) and NeuN (white) in control condition and cocultured with microglia cells. Scale bar 100 μm.

Figure S5 refers to Figure 4-5. IL-6 does not affect glutamatergic transmission at later stages of neuronal development and classical signaling is the predominant mechanism of IL-6 action in developing neurons.

(A) Schematic diagram of the experimental procedure. Cultured cortical neurons were incubated with IL-6 10ng/ml at 1 and 4 DIV and (after a washout at 7 DIV) glutamatergic synaptic basal transmission was then assessed at 14 DIV. Right graphs: Quantification of mEPSCs frequency and amplitude in cortical neurons at 14 DIV. (Ctrl n=14, IL-6 n=15. Three independent experiments. *p= 0,0137 Mann-Whitney test).

(B) Schematic diagram of the experimental procedure. Cultured neurons were incubated with 10ng/ml IL-6 for 7 days, from 1 to 7 DIV (Upper scheme) or from 14 to 20 DIV (lower scheme) (adding IL-6 every 2 days) and then assessed for excitatory basal transmission through patch-clamp recording at 21 DIV. (Right panels) Quantification of mEPSCs frequency and amplitude in the indicated conditions. (Ctrl n= 35, IL-$6_{1\text{-}7DIV}$ n=28, IL-$6_{14\text{-}20DIV}$ n=30. Four independent experiments. Kruskal-Wallis test followed by Dunn's multiple comparisons test. ***p=0,0010, **p=0,0013).

(C) Representative traces of mEPSCs obtained from cultured hippocampal neurons at 14 DIV acutely perfused with vehicle for 1 minutes and with IL-6 10ng/ml for at least 5 minutes (here shown only 1 minutes). Lower graphs: quantification of frequency and amplitude of mEPSCs before and after the application of IL-6. (n=7 cells. Wilcoxon paired test).

(D) Schematic diagram of the experimental procedure. Cultured hippocampal neurons established from E18 or E15 embryonic brain were incubated with IL-6 10ng/ml at 1 and 4 DIV and glutamatergic synaptic basal transmission was then assessed at 14 DIV. Right graphs show the average mEPSCs frequency and amplitude in the two conditions. (Ctrl E15 n=8, IL-6 n=6, **p=0,004 Mann-Whitney test; Ctrl E18 n= 6, IL-6 E18 n=7, **p=0,0082 Mann-Whitney test, One independent experiment).

(E) Representative immunofluorescence images of cultured neurons at 7 DIV established from E18 and E15 and stained with GFAP (red), Map2 (green) and NeuN (white) and (F right panel) the relative quantification of the percentage of neurons (identified as NeuN-positive cells) and (F left panel) astrocytes (identified as GFAP-positive cells). E15 n=17, E18 n=17, astrocytes ****p=2,3 $x10^{-7}$, neurons **** p=2,3 $x10^{-7}$, Mann-Whitney test, one independent experiment).

(G) (Upper panel) Representative electrophysiological traces of mEPSCs recorded in cultured neurons at 14 DIV in control condition and upon a single application of distinct proinflammatory cytokines at 1 DIV (INFγ 25 ng/ml , TNFα 10 ng/ml , IL1β 40 ng/ml). (Lower panel) Quantification of mEPSCs frequency and amplitude in the indicated conditions. (ctrl n= 16 cells, INFγ n=14 cells, TNFα n=10, IL1β n=12 cells. Three independent experiments. One-way ANOVA on ranks followed by Dunn's multiple comparison test).

(H) Western blot analysis of STAT3 phosphorylation (left panel) in cortical tissue collected from embryos intraventricularly injected with either Vehicle or IL-6 for 3 hours. Quantification of the optical density of STAT3 phosphorylation in tyrosine 705 normalized versus STAT3 total protein amount. (Three independent experiments, Vehicle IV: n= 10 embryos. IL-6 IV n=11 embryos. **p=0,003. Unpaired T-test).

(I) Transcriptional expression of IL6R and gp130 in cultured neurons at 6 DIV in control condition and upon IL-6 application at 1 and 4 DIV. (five independent experiments. One sample t-test. *p= 0,0107).

(J) Western blot analysis of STAT3 phosphorylation in cultured neurons infected with lentivirus expressing scrambled shRNA or specific IL-6R shRNA, in control conditions and upon acute treatment (30 minutes) with IL-6 10 ng/ml.

(K) Time course transcriptional analysis of IL6R and gp130 in Ara-C-treated hippocampal neurons at 5, 10 and 15 DIV through qPCR (IL6R: five independent experiments, *p=0,0098; gp130: seven independent experiments, **p=0,0070. One sample t-test).

(L) Time course transcriptional analysis of IL6R (left panel) and gp130 (right panel) in hippocampi of embryos at different prenatal developmental stages (E16: n =3 from three litters; E18: n =3 from one litter, E19 n=3 from one litter, P0 n=3 from two litters. IL-6R: *p=0,039, Kruskal-Wallis followed by Dunn's multiple comparison test; gp130: *p=0,044. One way ANOVA One way ANOVA with Holm-Sidak's multiple comparison test).

(M) Time course transcriptional analysis of IL6R (left panel) and gp130 (right panel) in cortex of embryos at different prenatal developmental stages (E16: n =3 from three litters; E18: n =3 from one litter, E19 n=3 from one litter, P0 n=3 from two litters. IL-6R: *p=0,047. One way ANOVA with Holm-Sidak's multiple comparison test).

(N) Western blot analysis of STAT3 phosphorylation in cultured neuron at 7 DIV acutely treated (30 minutes) with IL-6 10ng/ml in the absence and presence of increasing concentrations of sgp130 (1,5 and 10 µg/ml).

(O) Western blot analysis of STAT3 phosphorylation in macrophage cell lines RAW 264.7 acutely treated (30 minutes) with IL-6 10ng/ml in the absence and presence of sgp130 at 10 µg/ml.

(P) ELISA quantification of soluble IL-6R in supernatants of Raw 264.7 and hippocampal cultures, collected at indicated timepoints. (Raw 264.7 n=2, 7 DIV n=3, 14 DIV n=3, 30 DIV n=2).

Figure S6 refers to Figure 4-6: Role of different pro-inflammatory cytokines in glutamatergic synaptogenesis. Effect of Stattic dosage on neuronal death and glutamatergic synaptic transmission in developing cultures. The increase of STAT3 protein expression level is transient and is not due to STAT3 phosphorylation itself.

(A) Schematic representation of the experimental procedure used in Figure 6 C,D

(B) Neuronal death assay performed in neuronal cultures incubated at 1 DIV with different concentrations of Stattic (0; 0,5; 1; 2; 4 μM) using Calcein (live cells, green), Propidium Iodide (death cells, red) and *Hoechst* (total cells, in blue) in vivo staining. Scale bar 100 μm. (Lower panel) The percentage of dead (PI positive cells) and (Right panel) live cells (calcein positive cells) were evaluated as percentage of the total number of cells (*Hoechst positive cells)* (n= 9-15 coverslips analyzed for each condition. Roughly 100 cells analyzed for each coverslip. Three independent experiments. Kruskal-Wallis test. Calcein: **p=0,0059, ****p=5,5 x 10^{-6}; PI: **p=0,0019; ****p=3,2x10^{-6}).

(C) Representative traces of mEPSCs recorded in cultured neurons at 14 DIV in control condition and upon a single incubation of Stattic 1μM at 1 DIV. (Lower panel) Quantitative analysis of mEPSCs frequency and amplitude in the two conditions. (Ctrl n= 22 cells, IL-6 n=18 cells. Three independent experiments. Mann Whitney test).

(D) Scheme of *the* experimental procedure. IL-6 was chronically applied throughout the in vitro development of hippocampal neurons*,* from 1 DIV up to 13 DIV, by adding the cytokine with either Vehicle or Stattic 1 μM every 3 days.

(E) Representative traces of mEPSCs recorded in neuronal cultures at 14 DIV in the indicated conditions.

(F) Quantitative analysis of mEPSCs frequency and amplitude in the indicated conditions. (Ctrl n=22 cells, IL-6 n=26 cells, IL-6 Stattic n=31 cells. Four Independent experiments. One-way ANOVA on ranks followed by Dunn's multiple comparison test. Ctrl vs IL6 ***p=0,0004; IL-6 vs IL-6 Stattic***p=0,0002).

(G) Upper panel: western blot analysis of STAT3 protein expression in cultured neurons at 14 DIV chronically treated with IL-6 together with either Vehicle or Stattic 1 μM every 3 days (refer to scheme in D). Lower panel: quantification of the optical density of total amount of STAT3 protein in the different conditions normalized by the total amount of GAPDH protein (Three independent experiments, One sample t test *p<0,05).

(H) Western blot analysis of a panel of synaptic and non-synaptic proteins (left panel) evaluated in cultured neurons at 14 DIV in control condition and upon chronic treatment of IL-6 with the relative quantitative analysis (right) normalized by the total amount of GAPDH protein level. (Four independent experiment, One simple t test. *p<0,05).

(I) Schematic representation of the experimental procedure (Upper panel). IL-6 10ng/ml was incubated at 1 and 4 DIV (similar to scheme in Figure 4A), cultured neurons were then collected at 14 DIV and STAT3 expression was analyzed through western blot analysis (Right panel). STAT3 protein expression was normalized by total GAPDH protein. (Three independent experiments, Mann Whitney test).

Figure S7 refers to Figure 6. *Dose-effect* relationship of Galiellalactone and CCG-063802 on neuronal death in cultured neurons. Cluster identification methodology and predictive analysis of Rgs4 promoter region.

(A) Neuronal death assay performed in cultured neurons incubated with different concentrations of Galiellalactone (0; 2; 4; 8; 16 μM) at 1 DIV using Calcein (green), Propidium Iodide (red) and *Hoechst* (blue) in vivo staining. Scale bar 100 μm. (Right panel) the percentage of dead (PI positive cells, left panel) and live cells (calcein positive cells, right panel) were evaluated as percentage of the total number of cells (*Hoechst positive cells)* (n= 10-12 coverslips analyzed for each condition. Roughly 100 cells analyzed for each coverslip. Three independent experiments.). One-way ANOVA on ranks followed by Dunn's multiple comparison test. PI: ****p=0,00007; Calcein: ****p=0,00007.

(B). Western blot analysis STAT3 Phosphorylation at Tyrosine 705 in control condition and upon acute stimulation (30 min) of IL-6 in the presence of either Vehicle or Galiellalactone at 1 and 4 μM.

(C) Representative traces (left panel) of mEPSCs recorded in cultured neurons at 14 DIV treated with Galiellalactone 4 μM, at 1 DIV, and (right panel) the relative quantitative analysis (Ctrl n= 13 cells, Gall4 n= 15 cells. Three independent experiments. Mann Whitney test)

(D) Experimental workflow used for Figure 6J-K: cultured neurons were incubated with IL-6 for a short period (1 and 4 DIV) together with either vehicle or Galiellalactone and analyzed through patch-clamp recording at 14 DIV

(E) Experimental workflow used for single cell sequencing: cultured neurons were treated with IL-6 at 1 and 4 DIV, and subsequently dissociated at 6 DIV for the analysis.

(F) Feature violin plots showing gene modules score analysis for different cell types: CA-ExN; CA-Excitatory Neurons; CA-CR, CA-Cajal Raetzius; DG-ExN; DG- Excitatory neurons; InhN, Inhibitory Neurons; Astro, Astrocytes.

(G) Predicted Stat3 response element in the promoter of Rgs4, together with score and position. JASPAR^{2018} scan tool was used to assess enrichment. Only hits with a relative profile score threshold above 80% was considered significant.

(H) Experimental workflow used in Figure 7K-L: cultured neurons was incubated with IL-6 in the presence or absence of CCG-063802.

(I) Neuronal death assay performed in neuronal cultures incubated with different concentrations of CCG-063802 (0; 1,25; 2,5; 5; 7,5; 15 μM) a 1 DIV using Calcein (green), Propidium Iodide (red) and *Hoechst* (blue) in vivo staining. Scale bar 100 μm. (Right panel) The percentage of dead (PI positive cells, left panel) and live cells (calcein positive cells, right panel) were evaluated as percentage of the total number of cells (*Hoechst*

positive cells) (n= 9-18 coverslips analyzed for each condition. Roughly 100 cells analyzed for each coverslip. Three independent experiments.). One-way ANOVA on ranks followed by Dunn's multiple comparison test. PI: **p=0,0048, 7.5µM ****p=6,67x10^{-5}, 15µM ****p=9,84 x10^{-9}; Calcein: **p=0,0048, 7.5µM ****p=6,67x10^{-5}, 15µM ****p=9,84 x10^{-9}).

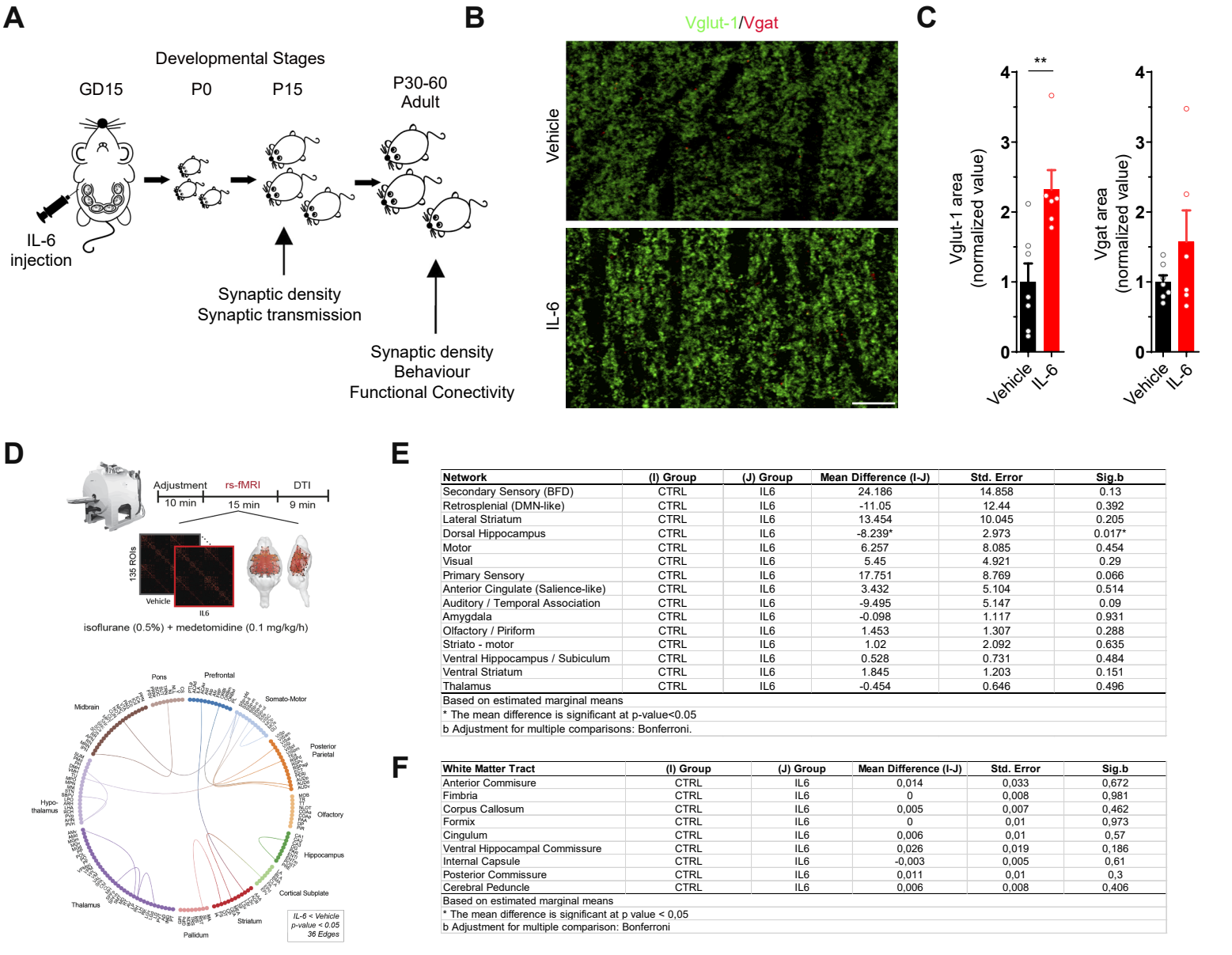

E

Network	(I) Group	(J) Group	Mean Difference (I-J)	Std. Error	Sig.b
Secondary Sensory (BFD)	CTRL	IL6	24.186	14.858	0.13
Retrosplenial (DMN-like)	CTRL	IL6	-11.05	12.44	0.392
Lateral Striatum	CTRL	IL6	13.454	10.045	0.205
Dorsal Hippocampus	CTRL	IL6	-8.239*	2.973	0.017*
Motor	CTRL	IL6	6.257	8.085	0.454
Visual	CTRL	IL6	5.45	4.921	0.29
Primary Sensory	CTRL	IL6	17.751	8.769	0.066
Anterior Cingulate (Salience-like)	CTRL	IL6	3.432	5.104	0.514
Auditory / Temporal Association	CTRL	IL6	-9.495	5.147	0.09
Amygdala	CTRL	IL6	-0.098	1.117	0.931
Olfactory / Piriform	CTRL	IL6	1.453	1.307	0.288
Striato - motor	CTRL	IL6	1.02	2.092	0.635
Ventral Hippocampus / Subiculum	CTRL	IL6	0.528	0.731	0.484
Ventral Striatum	CTRL	IL6	1.845	1.203	0.151
Thalamus	CTRL	IL6	-0.454	0.646	0.496

Based on estimated marginal means
* The mean difference is significant at p-value<0.05
b Adjustment for multiple comparisons: Bonferroni.

F

White Matter Tract	(I) Group	(J) Group	Mean Difference (I-J)	Std. Error	Sig.b
Anterior Commisure	CTRL	IL6	0,014	0,033	0,672
Fimbria	CTRL	IL6	0	0,008	0,981
Corpus Callosum	CTRL	IL6	0,005	0,007	0,462
Formix	CTRL	IL6	0	0,01	0,973
Cingulum	CTRL	IL6	0,006	0,01	0,57
Ventral Hippocampal Commissure	CTRL	IL6	0,026	0,019	0,186
Internal Capsule	CTRL	IL6	-0,003	0,005	0,61
Posterior Commissure	CTRL	IL6	0,011	0,01	0,3
Cerebral Peduncle	CTRL	IL6	0,006	0,008	0,406

Based on estimated marginal means
* The mean difference is significant at p value < 0,05
b Adjustment for multiple comparison: Bonferroni

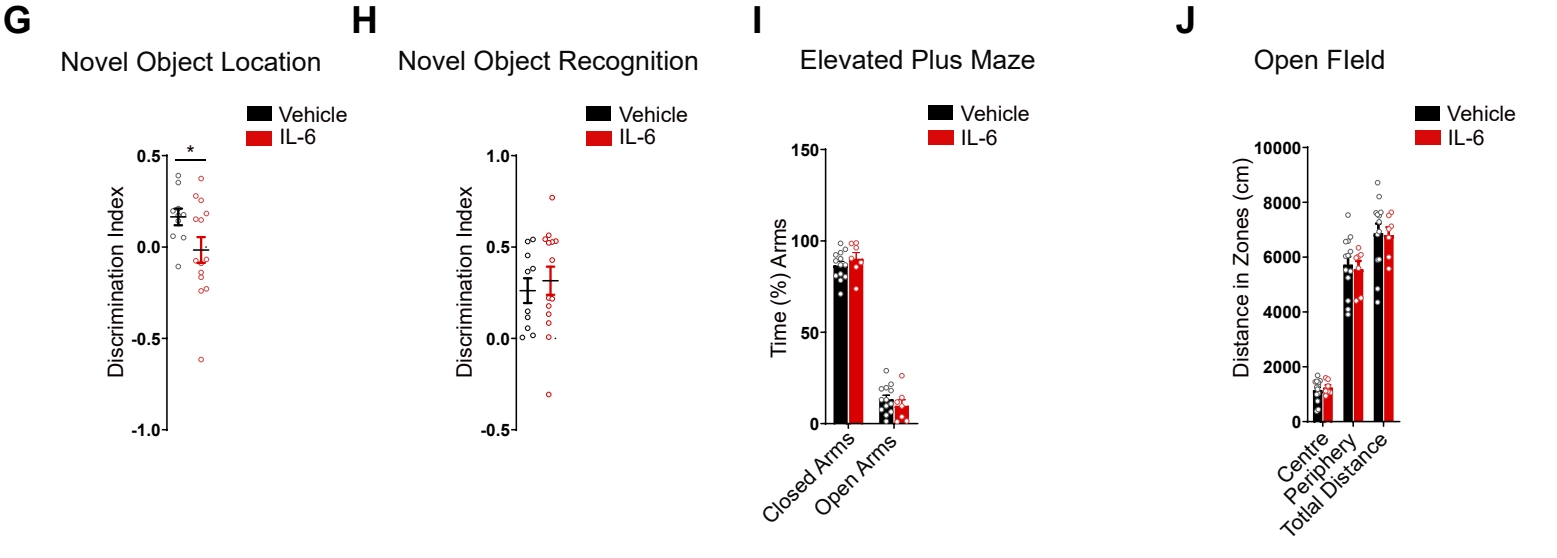

Mirabella et al., Figure S1

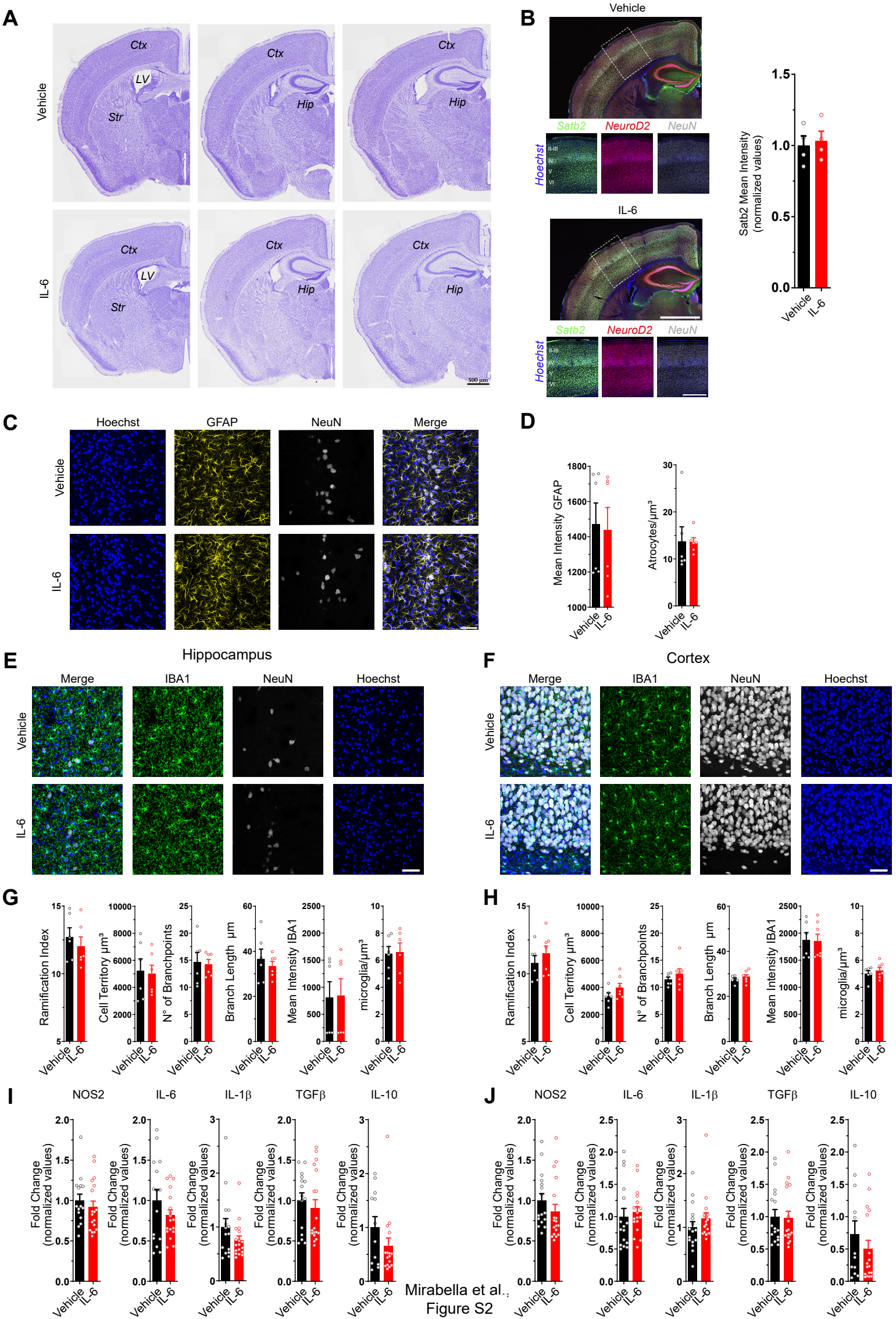

Mirabella et al., Figure S2

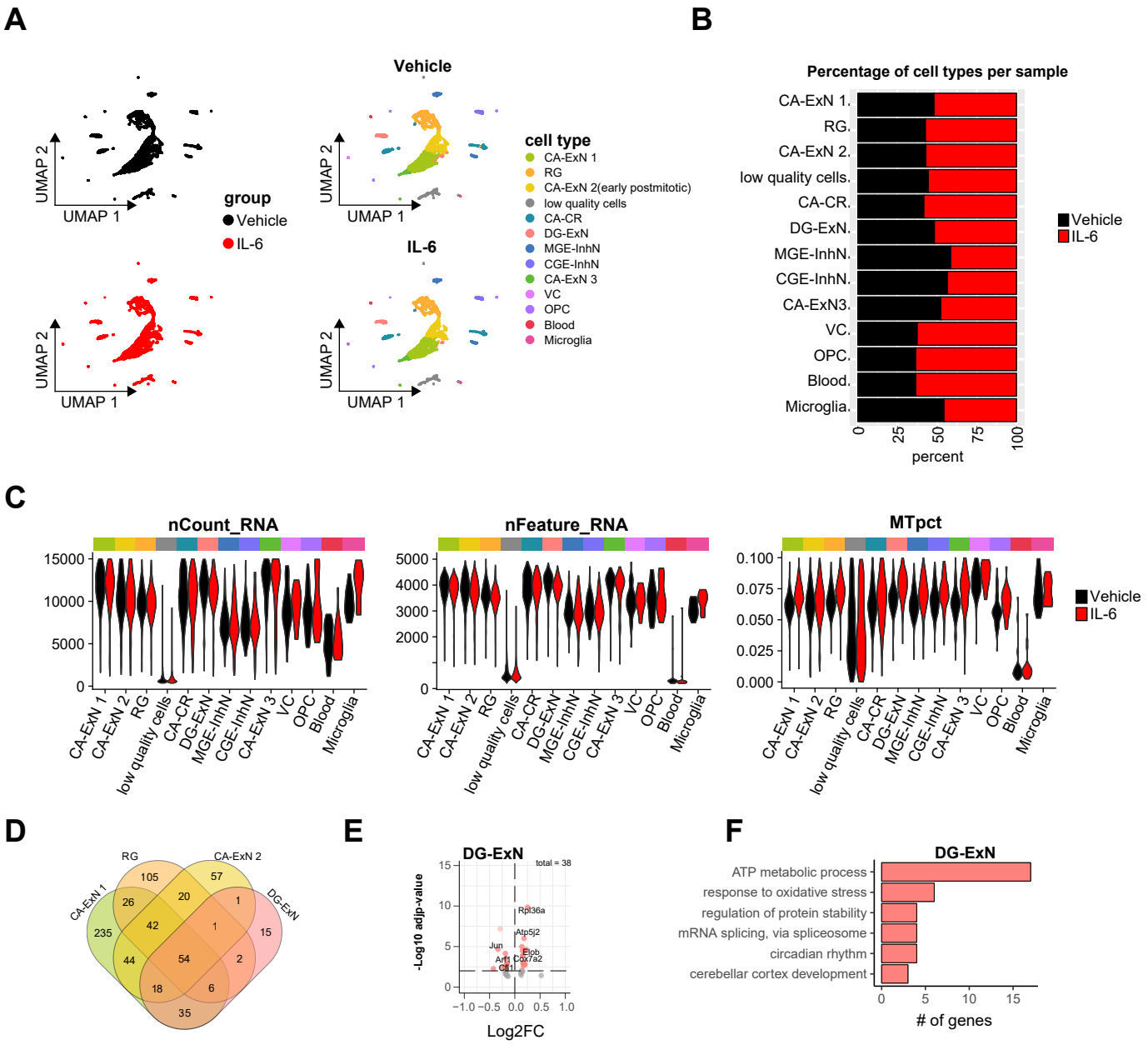

Mirabella et al., Figure S3

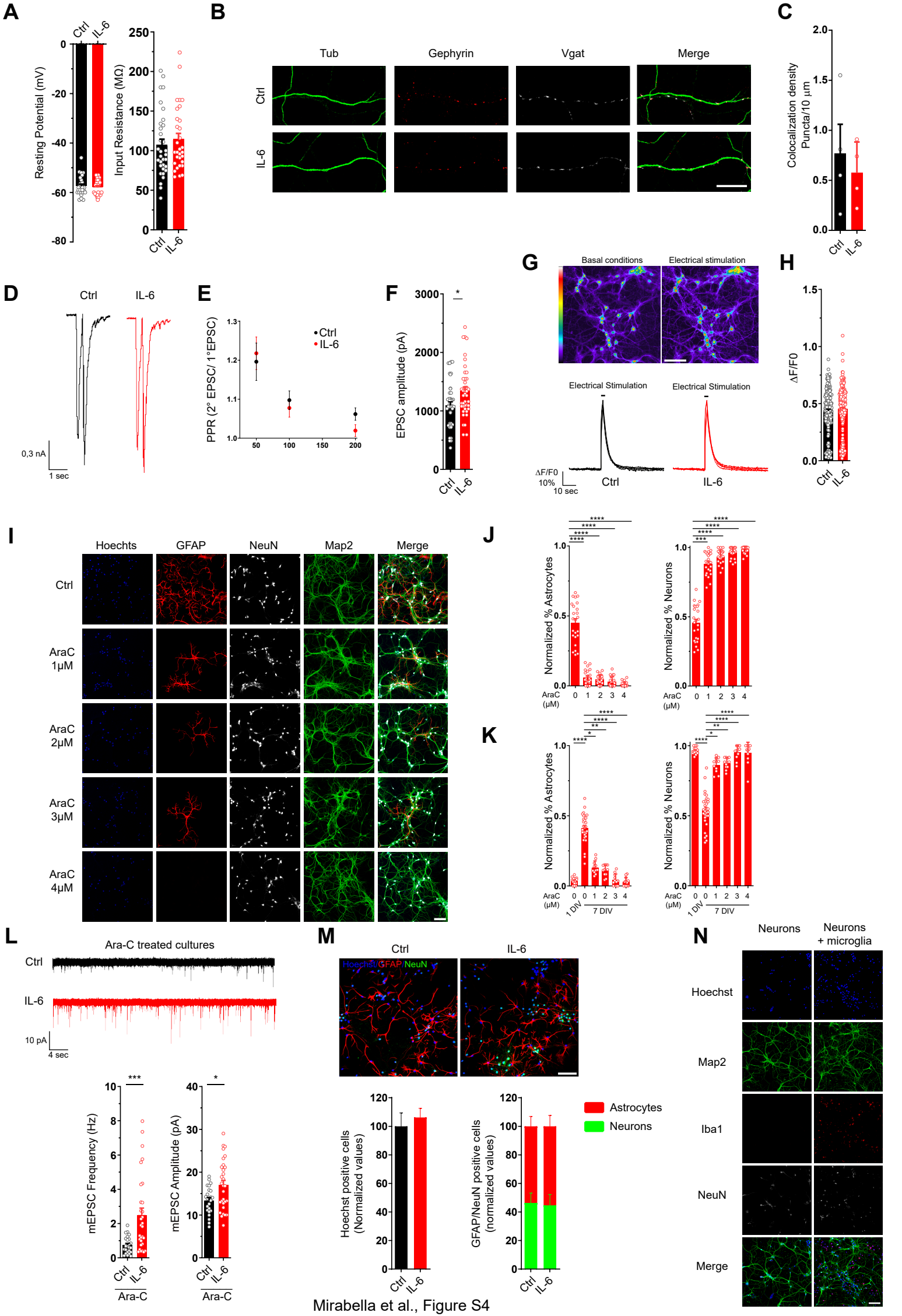

Mirabella et al., Figure S4

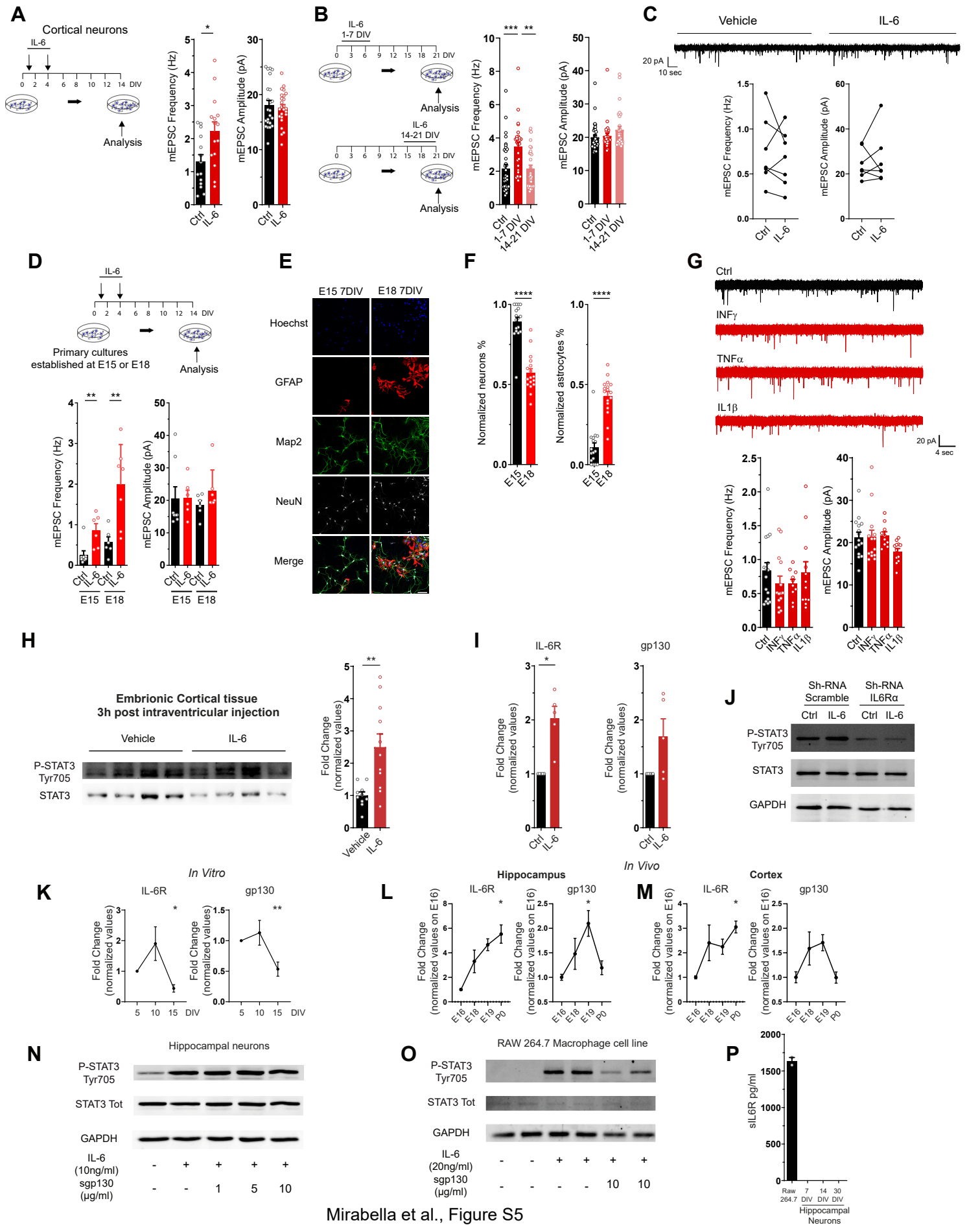

Mirabella et al., Figure S5

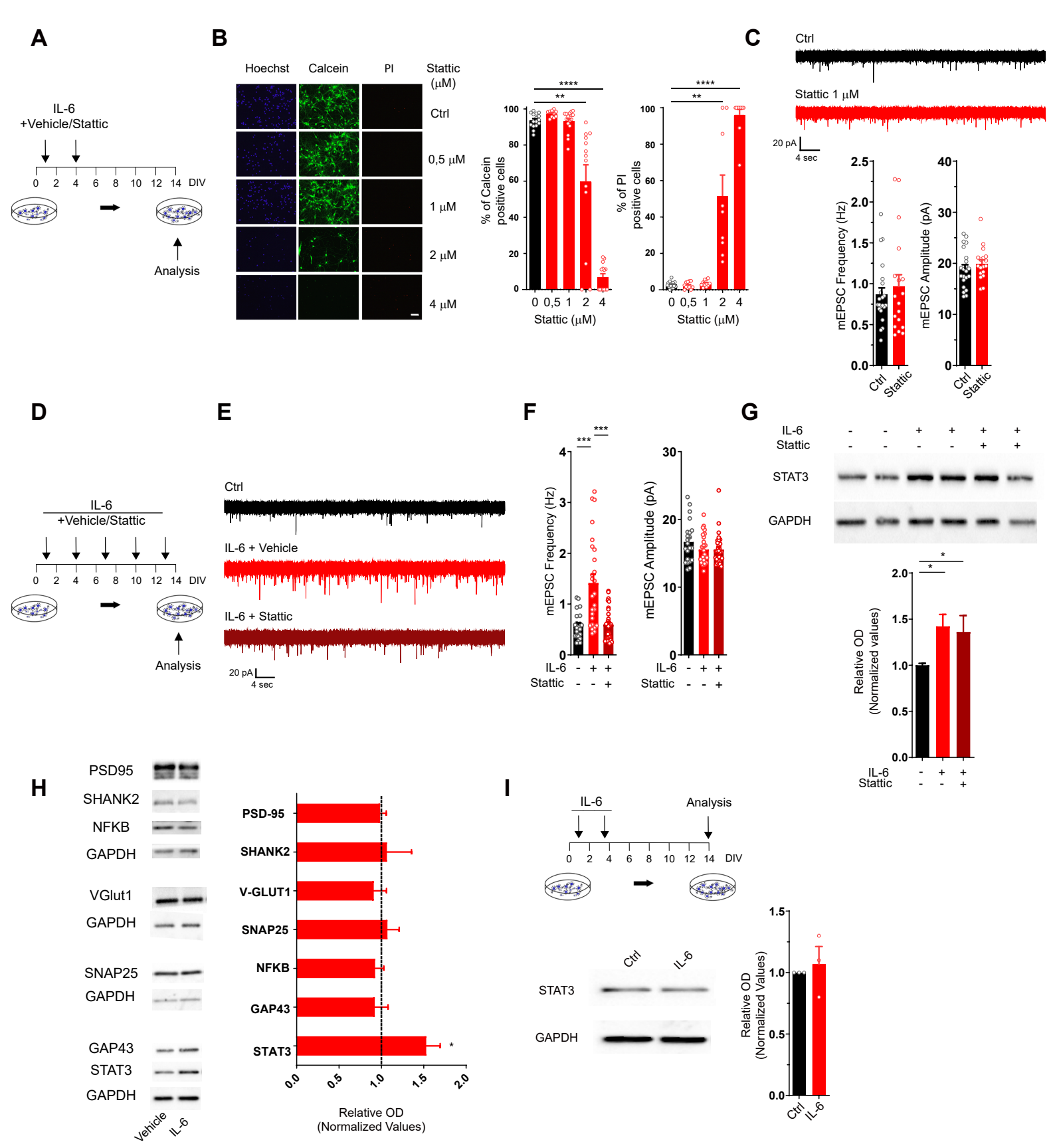

Mirabella et al., Figure S6

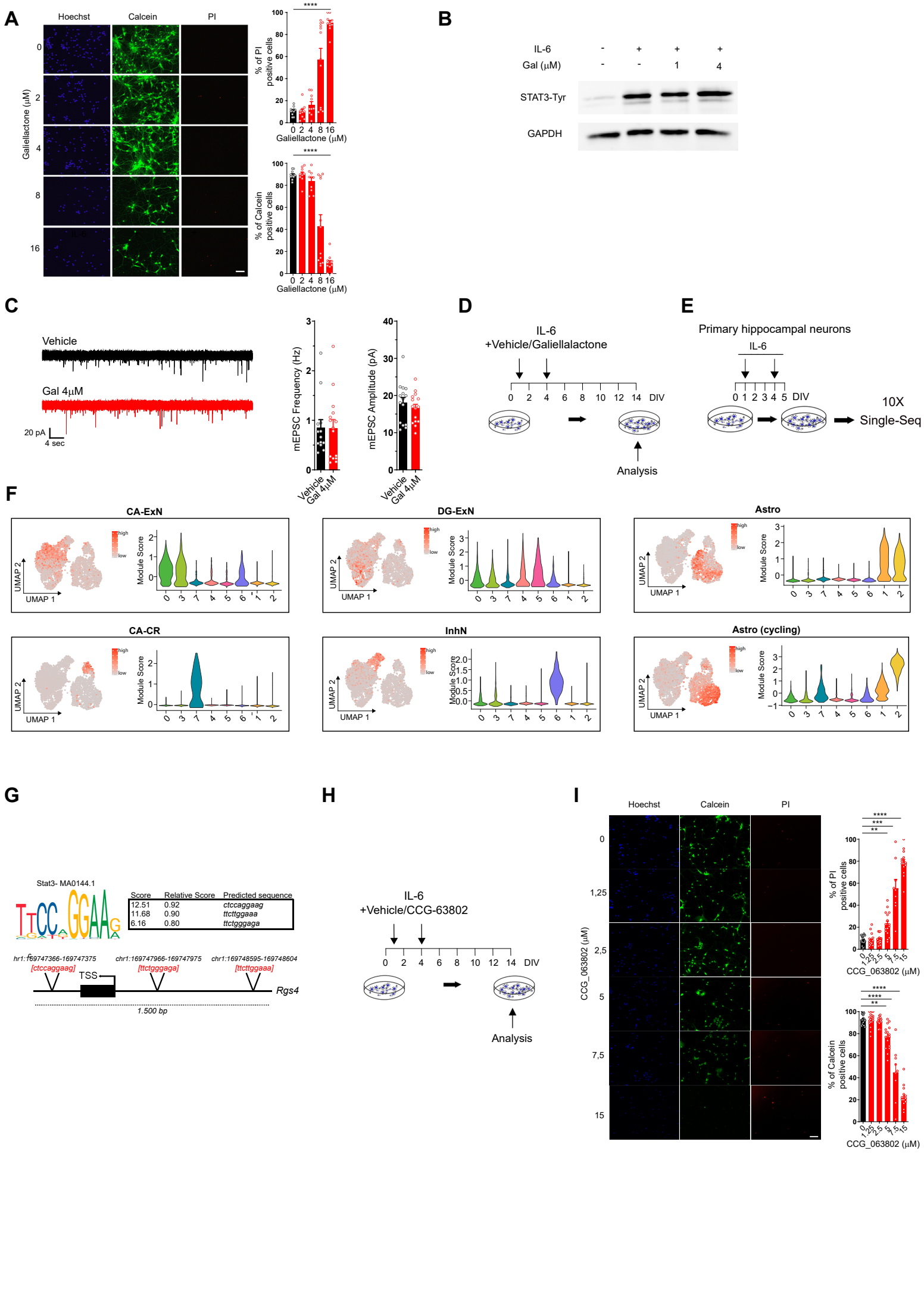

Mirabella et al., Figure S7